

Shrinkage forces due to polymerization of light-cured dental composite resin in cavities

Arakawa, Kazuo
Research Institute for Applied Mechanics, Kyushu University

<https://hdl.handle.net/2324/26047>

出版情報 : Polymer Testing. 29 (8), pp.1052-1056, 2010-12. Elsevier
バージョン :
権利関係 : (C) 2010 Elsevier Ltd.



Shrinkage forces due to polymerization of light-cured
dental composite resin in cavities

Kazuo Arakawa

Research Institute for Applied Mechanics, Kyushu University
Kasuga-koen 6-1, kasuga, Fukuoka 816-8580, Japan

ABSTRACT

A new method has been developed for determining shrinkage forces due to polymerization of light-cured dental composite resin in artificial cylindrical cavities. The cavities were fabricated in stainless steel plates, and shrinkage forces were measured using a load cell inserted in place of the floor of the cavity from the rear of the plate. The cavities were 3 mm in diameter, and depths varied from 0.5 to 3.5 mm to study the effect of light intensity. Cavities were filled with a composite resin after being prepared with a bonding agent and were then irradiated for 20 s with a light-curing unit at a power of 300 mW/cm². To study the effects of boundaries, two conditions were employed: a free surface condition without any restriction on the top surface of the cavity, and a constrained surface condition in which the top surface of the resin was bonded to a 1-mm-thick transparent polymethyl methacrylate (PMMA) plate. The shrinkage forces were measured as functions of time and the cavity depth, and the following results were obtained. For both conditions, the force increased with time, mostly during the irradiation stage (20 s) and then increased slightly after the irradiation. The force measured at 300 s increased gradually with the cavity depth and exhibited a maximum value before decreasing gradually. The cavities with constrained surfaces

yielded much greater shrinkage forces than those with the free surface condition for any given cavity depth.

Key words: Dental restorative material, Light-cured composite resin, Polymerization, Shrinkage force, Cavity depth

1. Introduction

Light-cured composite resins are widely used in dental restoration because of their ease in handling, esthetic appearance and minimal invasion of healthy tooth tissue. The wide use of composite resin has been prompted by the introduction of new resin products with good physical and mechanical properties as well as new bonding agents that adhere strongly to tooth tissue [1,2]. However, contraction stress due to polymerization shrinkage can reportedly damage or cause defects in the resin restoration and the tooth structure at the interface between the tissue and the restoration material. To avoid such damage or defects and to achieve better clinical treatments, polymerization shrinkage has, therefore, been widely studied using different experimental methods [3-25]. Feilzer et al. [4] studied the contraction stress observed when using specimens of composite resin inserted between two disks attached to a load cell. These experiments suggested that the contraction stress may depend on the ratio of the bonded area to the free non-bonded area of the specimens. Kinomoto et al. [6] and Kuroe et al. [10] examined contraction stress in simulated cavities using the photoelasticity method and reported that the intensity of the contraction stress depends

on the configuration of the cavity. The linear and volumetric shrinkage of composite resins have been measured using a dial gauge or a non-contact displacement sensor [15-20], and a dilatometer or gravimeter, respectively [21-23]. The laser speckle method has also been used to observe the shrinkage behavior of the composite resin [24]. However, shrinkage behavior in cavities and its relationship to the duration of light irradiation has not been investigated. Hence, from a clinical viewpoint, clarifying the shrinkage behavior in cavities generated by the polymerization process is very important.

We explored this issue by measuring the shrinkage behavior of composite resin using a digital image correlation method [26]. To simulate a clinical condition, cylindrical and semi-cylindrical cavities in bovine teeth were used to study the shrinkage behavior on the top free surface and simulated cross section, respectively. The shrinkage deformations in the cavities filled with the composite resin after preparation with a bonding agent were measured as functions of time. Several interesting points were observed concerning the shrinkage behavior. First, the displacement on the top surface increased and was concentrated near the center of the cavity as the irradiation time increased. Second, the center of the shrinkage moved gradually from the top surface to the floor of the cavity. Finally, such a movement of the center occurred mainly during the early stages of irradiation. We also evaluated the shrinkage behavior in the cavities using X-ray computerized tomography (CT) images and digital image correlation [27]. CT images captured before and after light curing by irradiation were recorded using fillers containing an X-ray contrast agent. The displacement distributions in the cavity were determined by applying a three-dimensional (3-D) alignment algorithm, and we

examined the shrinkage behavior of the resin to better understand the stress relaxation due to resin flow. The results showed that a large deformation was caused on the top free surface of the cavity, suggesting that this surface deformation can reduce the contraction stress or shrinkage force at the interface between the resin and the tooth structure.

This study examined the shrinkage force of a light-cured composite resin during polymerization using a load cell and cylindrical cavities fabricated in stainless steel plates. The cavities were made by inserting a load cell in place of the floor of the cavity, and various cavity depths were studied to investigate the effect of light intensity. The composite resin was poured into the cavity after spreading a bonding agent. The shrinkage forces were measured as functions of time and the cavity depth. As a reference, we also studied the shrinkage force under constrained surfaces by bonding the top surface of the resin to a transparent polymethyl methacrylate (PMMA) plate.

2. Materials and methods

The composite resin and the bonding agent used in this experiment were CLEARFIL AP-X and CLEARFIL tri-S BOND , respectively, supplied by Kuraray Medical Ltd. This material is a cross-linked acrylic resin composed of about 85 wt.% of inorganic powders and fillers. The relative compositions of these materials are listed in Table 1.

Figure 1 (a) shows a schematic diagram of a special device used to measure shrinkage forces that utilizes the lower half of a compact tensile testing machine constructed by the authors. This device consisted of a load cell for measuring the

shrinkage force, a stainless steel rod for connecting the load cell to the composite resin in the cavities, and a crosshead for mounting a stainless steel plate within the cavity. The steel plate was rigidly clamped on the upper part of the crosshead, which was able to move vertically.

Figure 1(b) shows the configuration for measuring the shrinkage force during the polymerization. Cylindrical cavities were constructed with a 5-mm-thick stainless steel (SUS304) plate with a hole 3 mm in diameter, and a stainless steel rod 2.9 mm in diameter that was inserted from the backside of the plate. We used this metal because it adheres readily to the composite resin. To study the effect of the light intensity on the cavities, we varied the depth of the cavities from 0.5 to 3.5 mm, shifting the location of the crosshead. Two boundary conditions of the cavities were employed: one a free surface condition without any restriction on the top surface of the cavity, and the other a constrained surface condition in which the top surface of the resin was bonded to a 1-mm-thick transparent PMMA plate. PMMA was used because it has similar properties to the composite resin and adheres readily to it.

The specimens were prepared using the following procedures: (i) the bonding agent was applied to the cavities after cleaning with ethanol, (ii) the cavities were irradiated for 10 s using a light-curing unit (Morita; JETLITE 3000) with a power of 300 mW/cm^2 , (iii) the composite resin was then poured into the cavities and its surface was ground flat. Under the free surface condition, the resin was irradiated with light directly, whereas under the constrained surface condition, a 1-mm-thick transparent PMMA plate with the bonding agent was placed on the top surface of the cavity and the light was irradiated

through the plate. In this experiment, the top surface was irradiated for 20 s at 10-mm from the light source, as is a common procedure in clinical practice. The shrinkage force was recorded over a 300-s period from the beginning of the irradiation.

3. Results

The shrinkage force P due to the polymerization was determined as a function of time t using the testing machine (see Fig. 1). Figure 2 shows three P - t diagrams for different cavity depths h under the free surface condition. P for $h=0.8$ mm increased greatly during the irradiation stage (20 s), and then slightly increased with t after the irradiation, resulting in $P=7.5$ N at $t=300$ s. P for $h=2.1$ mm showed a steep increase compared to P for $h=0.8$ mm and yielded $P=32$ N at $t=300$ s, while P for $h=2.4$ mm decreased than P for $h=2.1$ mm. The experimental data that exhibited noticeable decreases in P following irradiation were not included due to damage or defects at the interface between the resin and the cavity.

Figure 3 plots the shrinkage force P^* determined at 300 s after the start of the irradiation as a function of the cavity depth h . The value of P^* increased with h , reached its maximum value, and then decreased. Although there was scattering of the data, P^* showed a maximum value (32 N) around $h=2.1$ mm.

Figure 4 shows three P - t diagrams for different cavity depths h under the constrained surface condition. Similar to the free surface condition, P increased abruptly during the irradiation stage (20 s) and then gradually increased with t after the irradiation. As h increased from 0.7 to 1.3 mm, P increased greatly, whereas P decreased significantly

for $h=2.5$ mm, resulting in a similar situation to the free surface condition. However, P under the constrained surface condition yielded much larger values for a given depth.

Figure 5 shows the shrinkage force P^* at 300 s as a function of the cavity depth h . Similar to the result in Fig. 3, P^* increased with h and then decreased. The maximum value of P^* in Fig. 5 was about 70 N at approximately $h=1.6$ mm. This result indicated that the maximum value under the constrained surface condition was much greater than that observed under the free surface condition, and that the cavity depth which gave the maximum P^* value in Fig. 5 was attained earlier than that in Fig. 3.

4. Discussion

Figure 6 shows the comparison between two results determined under free and constrained cavity surfaces to study the effect of boundary conditions. As described earlier, the shrinkage force is much larger under the constrained surface condition for a given cavity depth. This suggests that the constrained surface decreases the flow of the resin from the top surface into the cavity and then caused displacement of the load cell resulting in a greater force. Therefore, the flow of the resin from the top surface into the cavity can decrease the contraction stress near the cavity floor. This result positively suggests that we can control the contraction stress at the interface between the resin and tooth structure, thereby minimizing interfacial damage or defects in the cavities.

The cavity depth giving the maximum P^* value in the constrained surface condition was smaller in comparison to that in the free surface condition. This shift can be

understood if one consider the attenuation of light intensity in the cavity due the PMMA plate on the top surface resulting in a lower degree of polymerization for a given depth.

In this experiment, a stainless steel rod connected to the load cell was inserted as a cavity floor before the shrinkage force of the resin was determined (see Fig. 1).

However, the shrinkage force can deform the steel rod and the load cell and this deformation can also affect the force itself measured by the load cell. Hence, it is important to understand the influence of the modulus of the cavity floor, which was examined in this study using the force P and displacement δ diagrams. Figure 7 shows P - δ diagrams for the steel rod (line OA), for the load cell (line OB), and for both (line-OC). In this analysis, we employed the maximum load ($P=70$ N) determined under the constrained surface condition, and the corresponding displacement ($\delta=3.1\mu\text{m}$) was estimated from the elastic moduli of the rod and the load cell. The modulus of the testing machine was disregarded because it had a much greater stiffness than the rod and the load cell.

The effect of the shrinkage force on the displacement of the cavity floor was examined using the P - δ diagrams in Fig. 7. In this analysis, we assumed that the cavity floor displaced δ upward due to the shrinkage force P (see Fig. 1), and we evaluated a virtual force required to move the cavity floor back to its original position $\delta=0$. The following procedures were used: (i) the line OC was rotated around line δC , and point δ' ($=2\delta$) was determined, (ii) the intersection C' between the vertical line from point δ' and the extension of line OC was determined, (iii) and this intersection was used to determine a force corresponding to the displacement $\delta=0$ of the resin. This limit value

of the shrinkage force is double the measured value of that under the restricted surface condition if the cavity floor is completely rigid. This indicated that the shrinkage force at the cavity floor of a tooth structure with a finite modulus is always smaller than the limit value. Hence, this suggests that contraction stress can be decreased in clinical practice if a resin with a low modulus is laminated on the cavity floor before a high modulus resin is poured into the cavity.

5. Conclusions

The shrinkage force resulting from the polymerization of a light-cured composite resin was measured using a load cell and artificial cylindrical cavities. To study the influence of the light intensity, we constructed cavities 3 mm in diameter with varying depths of 0.5 to 3.5 mm. The resin was poured into the cavity after spreading a bonding agent. The shrinkage force was measured as functions of time and the cavity depth. As a reference, we also measured the shrinkage force under constrained surfaces bonded to a transparent PMMA plate, and the following results were obtained:

- (1) The shrinkage force increased greatly during the irradiation stage and slightly increased following the irradiation.
- (2) The shrinkage force P^* determined at 300 s increased, reached its maximum value, and then decreased as the cavity depth increased.
- (3) Under the constrained surface condition, the shrinkage force P^* for a given depth was much greater than that observed under the free surface condition.

(4) The cavity depth giving the maximum P^* was less under the constrained surface condition.

Acknowledgments

This work was supported by the Ministry of Education, Culture, Sports, Science and Technology (MEXT) Japan, as part of the “Highly-Functional Interfaces Science: Innovation of Biomaterials with Highly Functional Interface to Host and Parasite” project. The author would like to express his gratitude to Mr. T.Mada from Kyushu University for his help in performing the experiments, Mr. S.Yamaguchi and Mr. Y.Takahata from Kuraray Medical Ltd. for their useful advice and for supplying the materials.

References

- [1] A. Peutzfeldt. Resin composites in dentistry the monomer systems. Eur J Oral Sci 1997; 105(2):97-116.
- [2] F.A. Rueggeberg. From vulcanite to vinyl, a history of resins in restorative dentistry. J Prosthet Dent 2002;87(4):364-79.
- [3] C.L. Davidson, A.J. Feilzer. Polymerization shrinkage and polymerization shrinkage stress in polymer-based restoratives. J Dent 1997;25(6):435-40.
- [4] A.J. Feilzer, A.J. De Gee, C.L. Davidson. Setting stresses in composites for two different curing modes. Dent Mater 1993;9:2-5.

- [5] D. Alster, B.A.M. Venhoven, A.J. Feilzer, C.L. Davidson. Influence of compliance of the substrate materials on polymerization contraction stress in thin resin composite layers. *Biomaterials* 1997;18(4):337-41.
- [6] Kinomoto Y, Torii M. Photoelastic analysis of polymerization contraction stresses in resin composite restorations. *J Dent* 1998;26(2):165-71.
- [7] Chen HY, Manhart J, Hickel R, Kunzelmann KH. Polymerization contraction stress in light-cured packable composite resins. *Dent Mater* 2001;17(3):253-9.
- [8] B.S. Lim, J.L. Ferracane, R.L. Sakaguchi, J.R. Condon. Reduction of polymerization contraction stress for dental composites by two-step light-activation. *Dent Mater* 2002;18(6):436-44.
- [9] D.C. Watts, A.S. Marouf, A.M. Al-Hindi. Photo-polymerization shrinkage-stress kinetics in resin-composites: methods development. *Dent Mater* 2003;19(1):1-11.
- [10] T. Kuroe, K. Tachibana, Y. Tanino, N. Satoh, N. Ohata, H. Sano, N. Inoue, A.A. Caputo. Contraction stress of composite resin build-up procedures for pulpless molars. *J Adhes Dent* 2003;5(1):71-7.
- [11] N. Ilie, K. Felten, K. Trixner, R. Hickel, K.H. Kunzelmann. Shrinkage behavior of a resin-based composite irradiated with modern curing units. *Dent Mater* 2005;21(5):483-9.
- [12] P.B. Bolhuis, A.J. de Gee, C.J. Kleverlaan, A.A. El Zohairy, A.J. Feilzer. Contraction stress and bond strength to dentin for compatible and incompatible combinations of bonding systems and chemical and light-cured core build-up resin composites. *Dent Mater* 2006;22(3):223-33.
- [13] F.C. Calheiros, M. Daronch, F.A. Rueggeberg, R.R. Braga. Influence of irradiant energy on degree of conversion, polymerization rate and shrinkage stress in an experimental resin composite system. *Dent Mater* 2008;24(9):1164-8.

- [14] J.R. Bausch, K. de Lange, C.L. Davidson, A. Peters, A.J. de Gee. Clinical significance of polymerization shrinkage of composite resins. *J Prosthet Dent* 1982;48:59-67.
- [15] M.P. Patel, M. Braden, K.W.M. Davy. Polymerization shrinkage of methacrylate esters. *Biomaterials* 1987;8:53-6.
- [16] E.L. DaBreo, P. Herman. A new method of measuring dimensional change. *J Prosthet Dentistry* 1991;65:718-22.
- [17] Watts DC, Cash AJ. Determination of polymerization shrinkage kinetics in visible-light-cured materials. *Dent Mater* 1991;7:281-7.
- [18] J. de Boer, R.J. Visser, G.P. Melis. Time-resolved determination of volume shrinkage and refractive index change of thin polymer films during photopolymerization. *Polym* 1992;33:1123-6.
- [19] B.A.M. Venhoven, A.J. de Gee, C.L. Davidson. Polymerization contraction and conversion of light-curing BisGMA-based methacrylate resins. *Biomaterials* 1993;14: 871–5.
- [20] V. Fano, I. Ortalli, S. Pizzi, M. Bonanini. Polymerization shrinkage of micro composites determined by laser beam scanning. *Biomaterials* 1997;18:467-70.
- [21] A.J. Feilzer, A.J. De Gee, C.L. Davidson. Increased wall-to-wall curing contraction in thin bonded resin layers. *J Dent Res* 1989;68(1):48-50.
- [22] M. Iga, F. Takeshige, T. Ui, M. Torii, Y. Tsuchitani. The relationship between polymerization shrinkage measured by a modified dilatometer and the inorganic filler content of light-cured composites. *Dent Mater J* 1991;10(1):38-45.
- [23] E. Asmussen, A. Peutzfeldt. Direction of shrinkage of light-curing resin composites. *Acta Odontol Scand* 1999;57:310-5.

- [24] T. Sato, M. Miyazaki, A. Rikuta. Real-time dimensional change in light-cured composites at various depths using laser speckle contrast analysis. *Eur J Oral Sci* 2004;112:538-44.
- [25] M. Atai, D.C. Watts, Z. Atai. Shrinkage strain-rates of Dent resin-monomer and composite systems. *Biomaterials* 2005;26:5015-20.
- [26] T. Furukawa, K. Arakawa, Y. Morita, M. Uchino. Polymerization shrinkage behavior of light cure resin composites in cavities. *J Biomech Sci Eng* 2009;4(3):356-64.
- [27] K. Arakawa, T. Furukawa, Y. Morita, M. Uchino, H. Kaida. Shrinkage behavior of a light cure resin composite in cavities. *J JSEM* 2010;10(Special issue):in press.

Figure captions

Fig. 1. Testing machine and surface conditions of cavities. (a) A schematic diagram of a special device for the shrinkage force measurement. (b) Free and constrained surface conditions for cavities.

Fig. 2. The shrinkage force P as functions of time and cavity depth under the free surface condition.

Fig. 3. The shrinkage force P^* after 300 s as a function of cavity depth under the free surface condition.

Fig. 4. The shrinkage force P as functions of time and cavity depth under the constrained surface condition.

Fig. 5. The shrinkage force P^* after 300 s as a function of cavity depth under the constrained surface condition.

Fig. 6. The shrinkage force P^* under the free and constrained surface conditions.

Fig. 7. Force P and displacement δ relationship for the testing machine.

Table

Table 1
The light-cured composite resin and the bonding agent used in this study.

Product name	Material	Conformation	Composition
kuraray CLEARFIL AP-X	resin	past	monomer (Bis-GMA, TEGDEMA) filler (glass powder, silica micro filler), etc.
kuraray CLEARFIL tri-S BOND	bonding agent	liquid	monomer (Bis-GMA, MDP, HEMA) ethanol, water, etc.

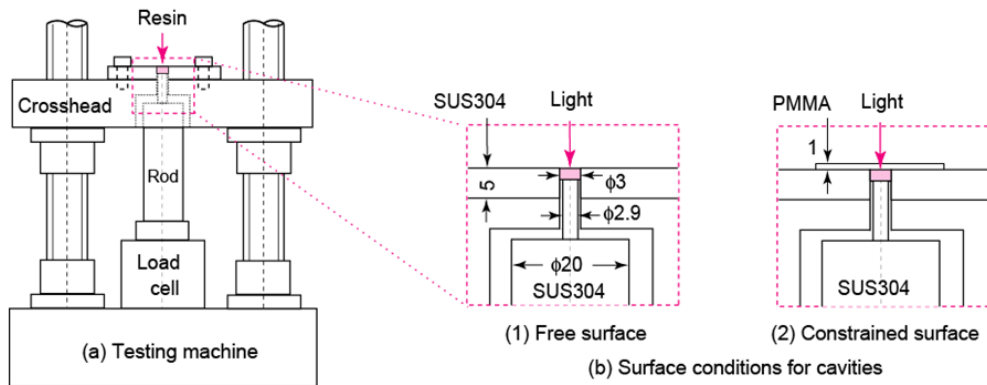


Fig. 1. Testing machine and surface conditions of cavities. (a) A schematic diagram of a special device for the shrinkage force measurement. (b) Free and constrained surface conditions for cavities.

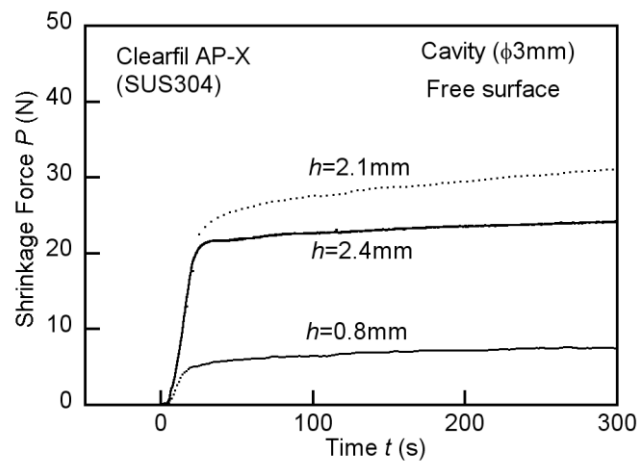


Fig. 2. The shrinkage force P as functions of time and cavity depth under the free surface condition.

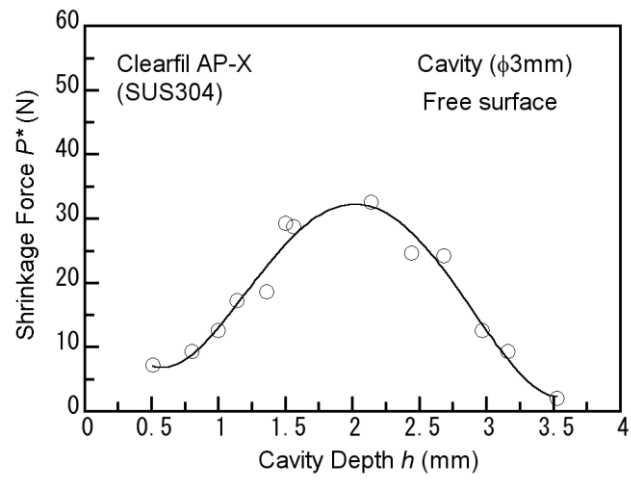


Fig. 3. The shrinkage force P^* after 300 s as a function of cavity depth under the free surface condition.

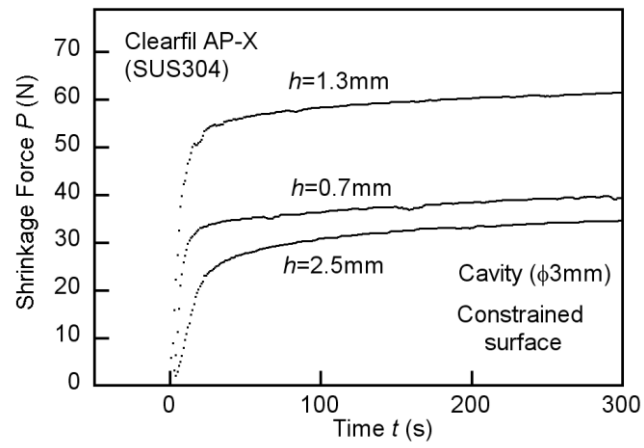


Fig. 4. The shrinkage force P as functions of time and cavity depth under the constrained surface condition.

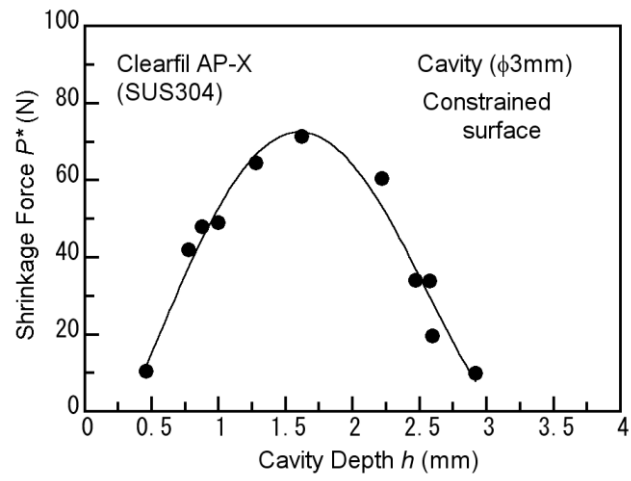


Fig. 5. The shrinkage force P^* after 300 s as a function of cavity depth under the constrained surface condition.

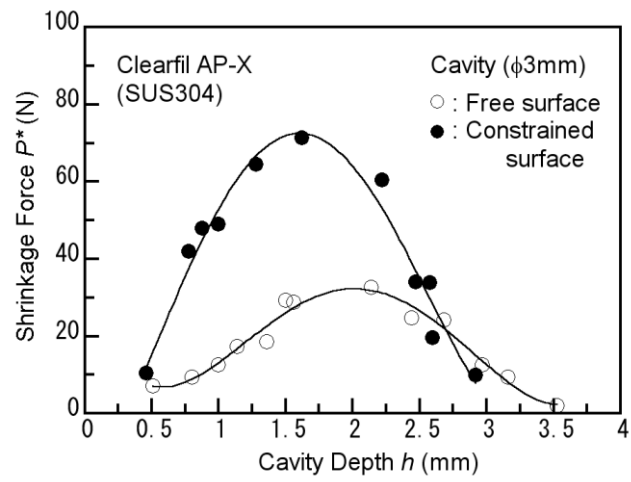


Fig. 6. The shrinkage force P^* under the free and constrained surface conditions.

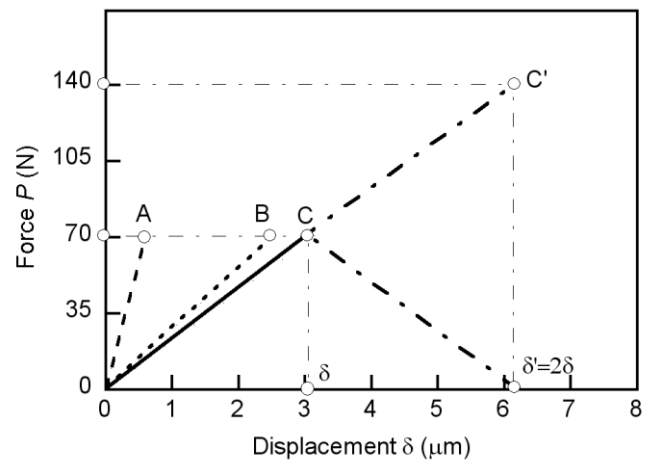


Fig. 7. Force P and displacement δ relationship for the testing machine.